Supplement of Nat. Hazards Earth Syst. Sci., 23, 3509–3523, 2023
https://doi.org/10.5194/nhess-23-3509-2023-supplement

Natural Hazards and Earth System Sciences
Open Access
EGU

Supplement of

Back analysis of a building collapse under snow and rain loads in a Mediterranean area

Isabelle Ousset et al.

Correspondence to: Guillaume Evin (guillaume.evin@inrae.fr)

S1 Additional information about the Irstea Cévennes building

This section gives some details about the Irstea Cévennes building. Figure S1 shows the geometric details (size and shape) of the metal structure of each facade of the Irstea Cévennes building.

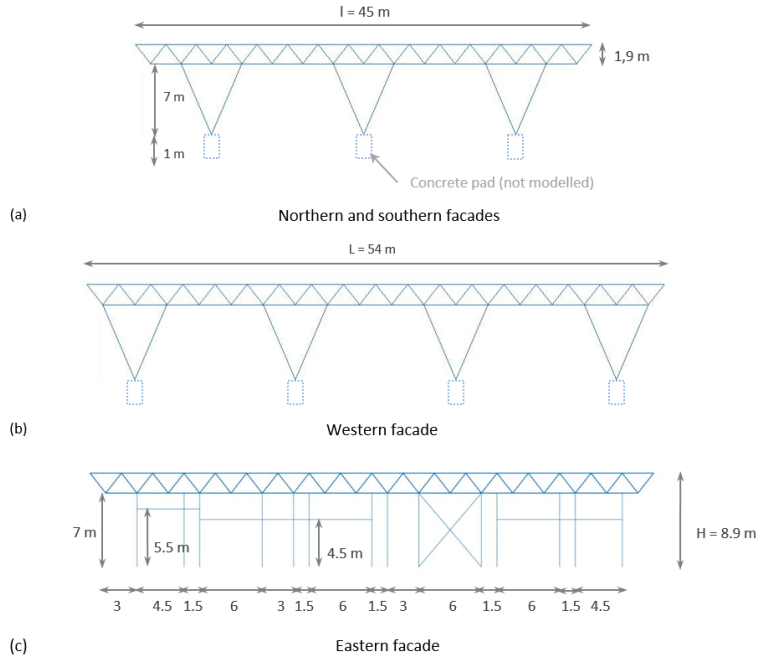

Figure S1. Sketches showing the geometric details (size and shape) of the metal structure of each facade of the Irstea Cévennes building.

Figure S2 provides the location map of the Cévennes building on the Montpellier site of Irstea (now INRAE).

Figure S2. Map of the Irstea Cévennes building in Montpellier. Source: INRAE.

The top panel of Figure S3 gives close-up views of the different types of damage to the structure of the Irstea Cévennes building, as observed on March 18, 2018, a few weeks after the roof collapse. The bottom panel of Figure S3 gives an overall description of the geometry of the metal structure with the exact location of each picture shown in the top panel.

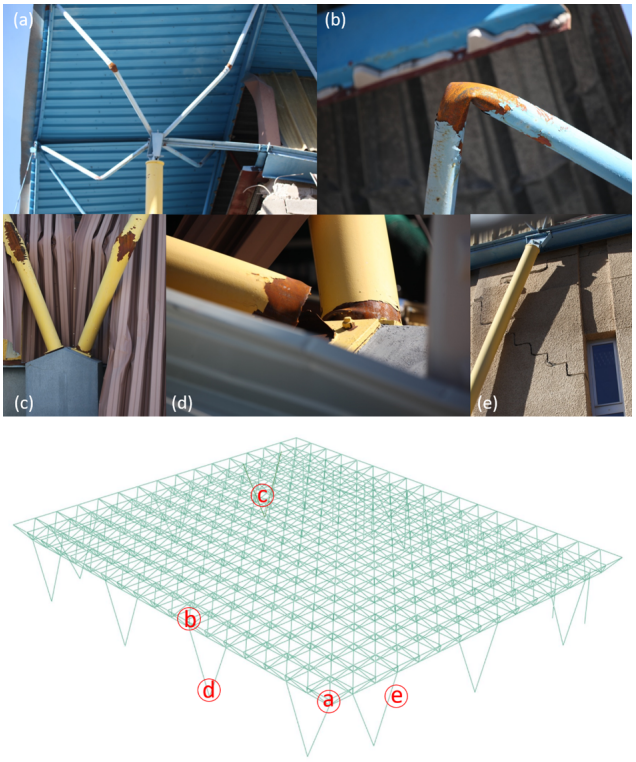

Figure S3. Close-up views of the damage to the structure of the Irstea Cévennes hall, as observed on March 18, 2018 (top panel): (a,b) buckling failures of roof tubular profiles, (c,d) bending and shear failures of tubular supporting pylons and (e) cracks in the concrete interior office walls located along the southern side of the building. Geometry of the metal structure as modeled in the Abaqus FE software, with the exact locations of the photos shown in the top panel (bottom panel).

Figure S4 gives the details of the geometry of each component of the metal structure. The numerical values assigned to the various geometric properties defined in Figure S4 are given in Table S1.

Figure S5 shows the rainwater drainage system of the Irstea Cévennes building, with a close-up view of one of the outlets. The slope of the roof is 1% on either side of a north-south peak line, allowing the water to flow to the outlets which are 20 cm high and located at the base of the low walls surrounding the roof. There are 7 outlets for rainwater drainage: 4 located in the corners, 1 in the middle of the western facade and 2 in the eastern facade (see Figure 6a in the main text).

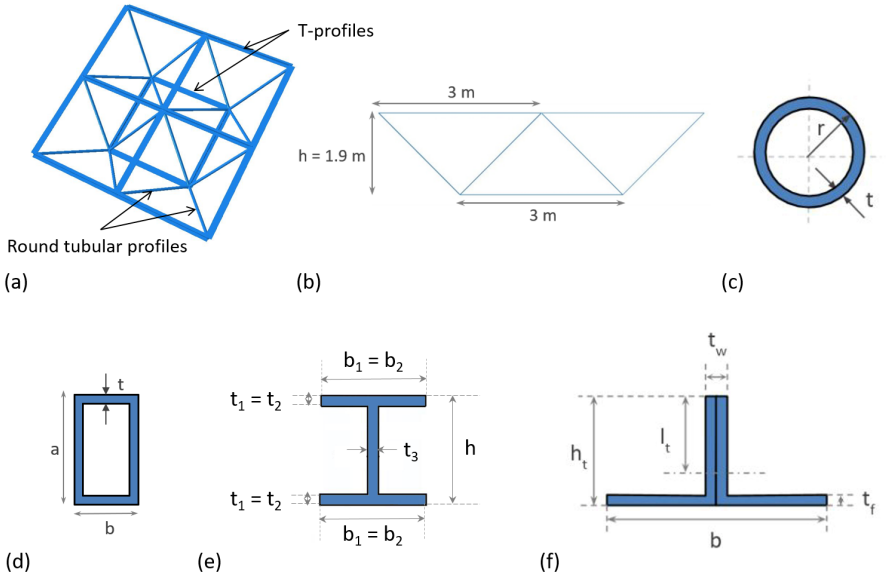

Figure S4. Details of the metal structure: general view (a) and front view of a single roof frame element (b), round (c) and rectangular (d) tubular profiles' and HEA (e) and T- (f) profiles' features.

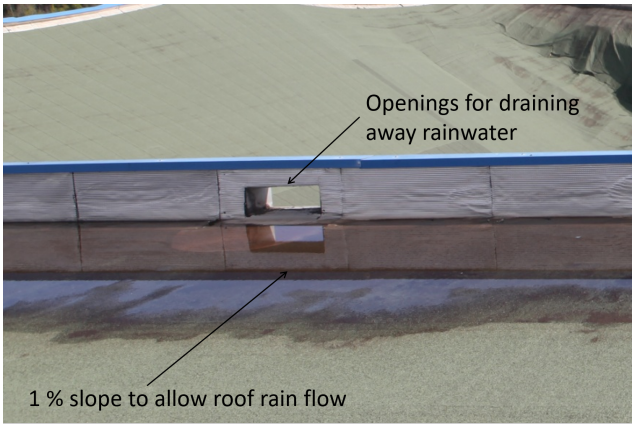

Figure S5. Roof rain drainage system of the Irstea Cévennes building: close-up view of one outlet for draining rainwater, with the indication of the 1% slope towards the outlet.

Table S1. Numerical values for the geometric properties of each element of the metal structure, as shown in Figure S4.

Parameter	Symbol	Value	Unit
Global structure			
Roof width	l	45.00	m
Roof length	L	54.00	m
Roof height	h	1.90	m
Total height	H	9.90	m
Top and (bottom) roof lattice T-profiles			
Width	b	160 (120)	mm
Height	h_t	100 (80)	mm
Thickness	t_f	9 (7)	mm
Thickness	t_w	18 (14)	mm
Position of the local cross-section axis	l_t	68.9 (54.5)	mm
HEA 160			
Width	$b_1 = b_2$	160	mm
Height	h	152	mm
Thickness	$t_1 = t_2$	9	mm
Thickness	t_w	6	mm
Round tubular profiles of roof lattice			
Outer radius	r	24.15	mm
Thickness	t	2.9	mm
Round tubular profiles of facades			
Outer radius	r	109.55	mm
Thickness	t	4.5	mm
Rectangular tubular profiles			
Height	a	100	mm
Width	b	50	mm
Thickness	t	2	mm

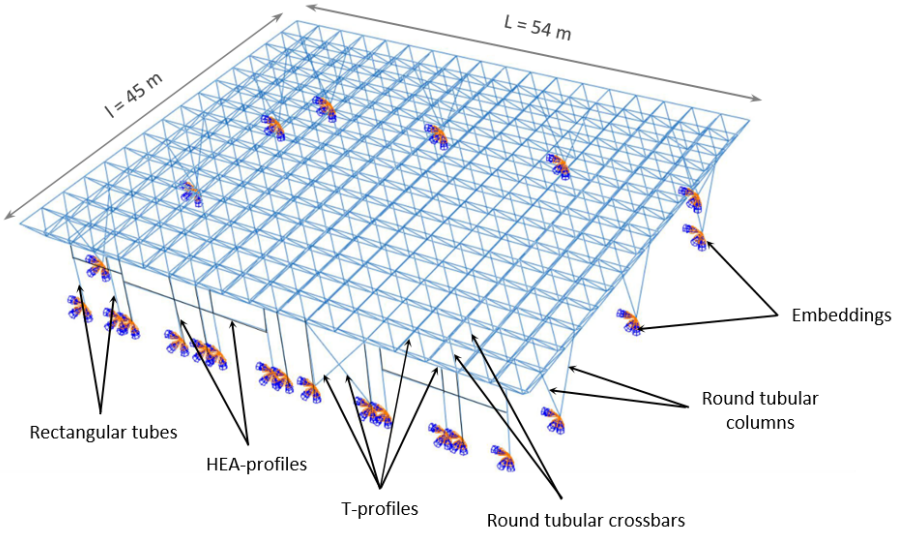

Figure S6. Overview of the metal structure of the Cévennes building modeled with the FE Abaqus software.

Table S2. Material properties considered in the FE model to describe the behavior of the entire structure.

Parameter	Notation	Unit	Value
Type	S235	-	-
Density	ρ_s	kg.m^{-3}	7850
Young modulus	E_y	MPa	210000
Poisson ratio	ν	-	0.3
Yield strength	f_y	MPa	294
Ultimate strength	f_u	MPa	432
Ultimate strain	ε_u	-	0.2

S2 Description of the finite element model

In order to investigate in detail the mechanical response of the Irstea Cévennes building and thus better understand its collapse under snow and rain loading, the metal supporting structure was modeled using the Finite Element (FE) software Abaqus (Dassault Systèmes, 2017). Figure S6 shows an overall sketch of the modeled structure in relation to the description of the building provided in the previous subsection. The details of the roof metal frame, which has been fully modeled by the FE-Abaqus, are shown in Figure S4. The dimensions of the structure and of all its components are given in Table S1. The structure is modeled in Abaqus by 132778 Timoshenko beam elements of type B31 (two-node linear beam element in space) type and 0.05 m long.

The Irstea Cévennes building dates from the 1980s, and the design records are not known precisely. The type of steel used in the supporting structure is unknown, and no material testing was carried out after the collapse. It is therefore assumed that the supporting structure was made entirely of S235 steel, which is commonly used in building construction. The behavior of the steel is described by a linear elasto-plastic law with strain hardening, which includes four parameters: Young's modulus E_y, yield strength f_y, ultimate strength f_u and strain ε_u. Their numerical values used in the FE simulations are given in Table S2. In the absence of post-collapse tests on steel elements, average values of steel strengths were used in the FE model based on the new Eurocode for the design of steel structures (CEN/TC250, 2022): f_y = 1.25 x 235 = 294 MPa and f_u = 1.2 x 360 = 432 MPa, together with an ultimate strain ε_u = 20 %.

Table S3. Line loads applied to the structure during the pushover FE simulations in the case of a uniform distribution for both water and rain.

Location of the T-profile	Roof weight [N.ml^{-1}]	Snow and rain weight [N.ml^{-1}]
Roof perimeter	45	0 to 3679
Inside the roof	90	0 to 7358

Table S4. Maximum values of applied line loads [N.ml^{-1}] on the structure during the pushover FE simulations in the cases of non-uniform snow and rain pressure distribution due to water accumulation at the edges and in the center of the roof, depending on the location of the T-profile (in accordance with the shape of the pressure profile given in Figure 7 of the main text).

	Edge accumulation			Central accumulation		
T-profile rebars location	NS	WE ext	WE int	NS	WE ext	WE int
A	6867	6867	13734	490.5	490.5	981
B	12753	5886	11772	1962	1471.5	2943
C	10791	4905	9810	3924	2452.5	4905
D	8829	3924	7848	5886	3433.5	6867
E	6867	2943	5886	7848	4414.5	8829
F	4905	1962	3924	9810	5395.5	10791
G	2943	981	1962	11772	6376.5	12753
H	1226.25	245.25	490.5	13488.75	7112.25	14224.5

The self-weight of the structure is considered using a steel density of $7\,850$ kg.m^{-3} (see Table S2). Two pressure fields are considered, corresponding to the self-weight of the sheet covering the lattice structure (not modeled) and the snow and rain induced loading. These are represented in the model by line loads (in N.ml^{-1}) applied on the entire upper T-profiles of the roof. The values of these line loads, identified in Tables S3 and S4, depend on whether the T-profile is located on the perimeter of the lattice or inside it, as well as on the choice retained for the distribution of the snow and rain pressure field.

The uniform pressure due to the self-weight of the sheet is taken to be 60 N.m^{-2} and converted to line loads as explained below for snow and rain loads.

As mentioned in the main text, three different cases of spatial distribution of snow and rain were studied: a uniform distribution, a case where water flowed rapidly at the edges of the roof, and a case where water accumulated mainly in the center of the roof. In the pushover simulations, the pressure applied to the structure is gradually and linearly increased until the structure fails. In the case of a uniform distribution, the pressure mimicking the snow and rain load introduced in the model is increased from 0 to a maximum pressure arbitrarily set at $4\,905$ N.m^{-2} (this last value is only used as an input in the FE model and is deliberately high in order to be able to observe the different failure criteria). In fact, the simulations stop as soon as the examined criterion is reached, well before this maximum pressure is reached. To convert this range of applied pressures (N.m^{-2}) into line loads (N.ml^{-1}), we consider the nominal length of a T-profile of the roof (3 m) and its position in the roof. With regard to the latter, two situations are taken into account: either the element is located at the edge of the roof (in which case, the T-profile carries a quarter of the load supported by a frame element 3 m $\times$ 3 m, see Figure S4a) or inside the roof (in which case, the T-profile is associated with two frame elements and carries twice a quarter of the load supported by a frame element 3 m $\times$ 3 m), as indicated in Table S3. In the other two cases, where we consider a non-uniform distribution of the applied water force over the area of the roof, the resulting line loads on the structure after rainfall are given in Table S4, based on the location of the T-Rebars mentioned in Figure S7 and in accordance with the pressure profiles shown in Figure 7 of the main text.

As the roof frame elements are not articulated in the real structure (in particular, round tubular profiles are welded to T-profiles), the roof frame has been modeled in one piece with rigid connections between the elements. The connections between the roof frame and the supporting tubular pylons are actually of a pivot type in the direction parallel to the facades in order to resist the wind. As the loads considered in the FE model are all vertical, this hinge should not be used. However, an FE model

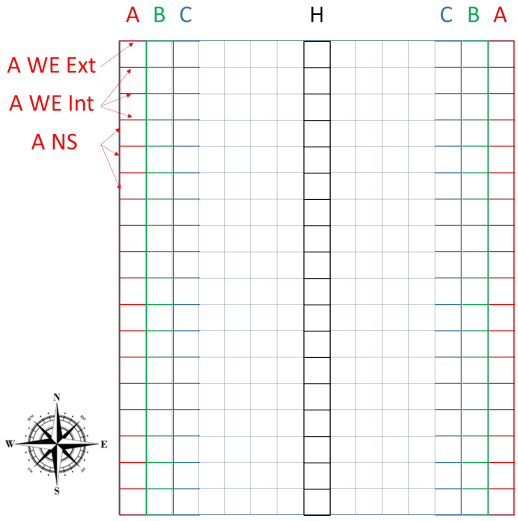

Figure S7. Location of T-bars affected by different snow and rain loads due to water accumulation either at the edges or in the center of the roof (see Table S4).

Table S5. Values of ground snow loads [N.m$^-$2] to be taken into account according to the French standard NV65, published in 1965, for Region II where the city of Montpellier is located.

Region	II
Normal overload	450
Extreme overload	750

with pivots was tested and both models gave similar results. A rigid connection between these elements was therefore taken into account in the model. Finally, all the columns of the facades are embedded.

S3 Analysis of the building collapse according to regulations

The existing regulation for snow load design in France at the time of the construction of the Irstea building in 1982 was the French standard defining the effects of snow and wind on buildings, originally published in 1965 (CGNG, 2000). This French standard was based on geographical areas (regions I, II, III and a region III + 45%) for which snow loads on the ground below 200 m above sea level were defined *a priori* and applicable to roofs not exceeding 25°. Table S5 gives the values of the ground snow loads that had to be taken into account for the design of buildings located in Region II, including the city of Montpellier.

Today, in compliance with Eurocode 1 and the standard NF EN 1991-1-3 adopted in France according to Eurocode 1 (CEN/TC250, 1991; AFNOR, 2004, 2007), the snow load on a roof, s, is defined by the following equation:

$$s = \mu_i \cdot C_e \cdot C_t \cdot s_o, \tag{S1}$$

where $s_o = s_k$ or s_{Ad}, and where s_k and s_{Ad} are the ground snow loads for permanent/transitional and accidental project situations, respectively (with respect to the geographical zone under consideration). μ_i is the roof shape coefficient, which takes into account undrifted and drifted snow loads, respectively, depending on the shape and slope of the roof. C_e is the exposure coefficient (equal to 0.8 for a windswept site, 1 for a normal site and 1.25 for a sheltered site). C_t is the thermal coefficient (equal to 1 for a roof without high thermal transmittance).

Table S6. Values of ground snow loads [N.m^{-2}] for the region where the city of Montpellier is located according to the NF EN 1991-1-3 standard published in 1991.

Region	B2
Characteristic value of ground snow load (s_k)	
at an altitude of less than 200 m	550
Design value of exceptional ground snow load (s_{Ad})	1 350

The ground snow load values to be applied in France are given for eight different zones depending on the altitude (the ones concerned in the present case are referred to in Table S6). They are determined on the basis of a probability of exceedance over a one-year period (excluding the case of exceptional snow) of 0.02 and assuming a snow density of 150 kg.m^{-3}. It should be noted that such a density value corresponds to relatively dry and fresh snow and is well below the typical density of wet snow (around 250 kg.m^{-3}), such as that involved in the present case study.

Eurocode 1 specifies that the roof snow load must be increased in areas where rain-on-snow can cause melting followed by frost, especially where snow and ice can block the roof drainage system. The NF EN 1991-1-3 standard stipulates that the roof snow load must be increased by 0.2 kN.m^{-2} if the water flow slope is less than 3 %, to take into account the increase in snow density due to the difficulty of draining water during rainfall.

In our case, the roof of the building consists of a single slope which is less than $30°$, only one load case is to be considered and $\mu_i = \mu_1 = 0.8$ for both permanent and accidental project situations with typical and exceptional snow loads, respectively.

Figure S8 compares the roof snow loads leading to the failure criteria of the Cévennes supporting structure according to the FE model simulations with the design values of the snow loads recommended by both regulations. As no safety factors have been considered in the FE simulations, a comparison is only made for design situations where the safety factors are equal to 1, *i.e.* the transient Serviceability Limit States (SLS) and the accidental Ultimate Limit States (ULS). Thus, in Figure S8a, the loads leading to the deflection and horizontal displacement limits are compared with the typical snow loads resulting from the French DTU NV65 standard (450 N.m^{-2}) and the NF EN 1991-1-3 standard, adopted in application of Eurocode 1 ($0.8\,\text{x}\,550 + 200 = 640$ N.m^{-2}) and in Figure S8b, the loads leading to material failure and buckling are compared with the design accidental snow loads resulting from both regulations (750 and $0.8\,\text{x}\,1\,350 + 200 = 1\,280$ N.m^{-2} respectively).

In these situations, we see that the building begins to fail in serviceability (Figure S8a) and yield (Figure S8b, orange bar) at snow loads well or just above the recommended design loads (in magenta and blue). In contrast, the load leading to buckling (non-linear buckling limit in brown in Figure S8b) is below the recommended accidental design loads of DTU NV65 and Eurocode 1 (in magenta and blue), and the theoretical linear buckling load (in beige) is also below the accidental design load recommended by Eurocode, but above the accidental design load recommended by DTU.

In France, the consideration of imperfections in the design of metal structures was introduced in the regulations in 1983, with the publication of the first version of the Regulation on Metal Construction, *i.e.* after the construction of the building studied here. If the initial geometric imperfections are not taken into account (linear buckling limit), the results show that the structure begins to be damaged by snow loads (equal to 930-940 N.m^{-2}) well above the extreme design load based on the DTU NV65, which is 750 N.m^{-2}. It therefore appears that the design of this building was carried out in accordance with the state of the art at the time (considering the limit states studied: transient SLS and accidental ULS, but not transient ULS).

Under the current regulations, taking into account initial geometric imperfections, buckling occurs first at a load of 645 N.m^{-2}, which is well below the Eurocode accidental design snow load (corresponding to a snow load of $1\,280$ N.m^{-2}). It is therefore clear that this structure did not comply with the current design basis rules. Note also that the estimated value for the snow-water mixture load of $1\,226 - 1\,325$ N.m^{-2} was equivalent to this exceptional snow load specified in the Eurocode.

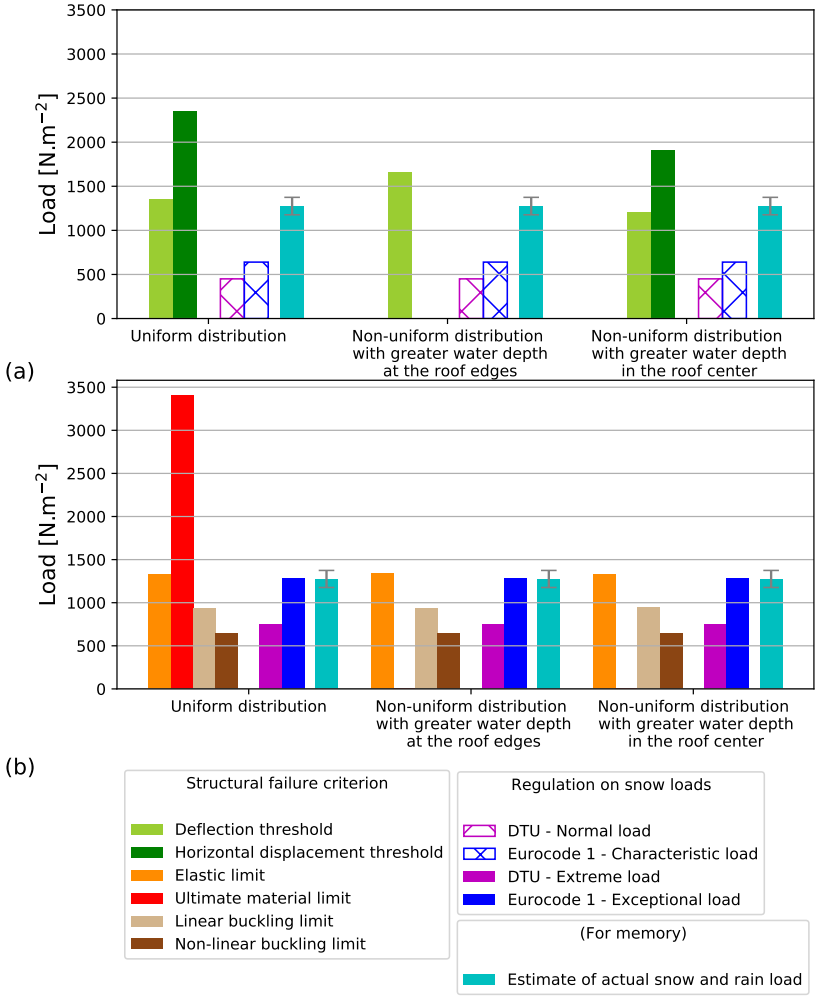

Figure S8. Comparison between the loads leading to the different failure criteria of the Cévennes building, as calculated by the FE model, and the snow load values recommended by Eurocode 1 and the DTU NV65 in the different cases of snow and rain pressure field for the transient SLS (a) and for the accidental ULS (b). The structure does not comply with the design basis rule if the design snow and rain load recommended by the regulation (in magenta and blue on the right, for each assumption of snow and rain distribution) is greater than a calculated failure load (on the left). The actual snow and rain load (in cyan on the right) is shown for information.

References

AFNOR: NF EN 1991-1-3 : Eurocode 1 : Actions sur les structures - Partie 1-3 : Actions générales - charges de neige, Association Francaise de Normalisation (AFNOR), 2004.

AFNOR: NF EN 1991-1-3/NA : Eurocode 1 : Actions sur les structures - Partie 1-3 : Actions générales - charges de neige. Annexe nationale à la NF EN 1991-1-3, Association Francaise de Normalisation (AFNOR), 2007.

CEN/TC250: Eurocode 1: Actions on structures - Part 1-3: General actions - Snow loads (EN 1991-1-3), Comité européen de Normalisation / Comité Technique CEN/TC 250 "Eurocodes structuraux", 1991.

CEN/TC250: Eurocode 3 - Design of steel structures - Part 1-1: General rules and rules for buildings (FprEN 1993-1-1:2023, CEN/TC 250 - Structural Eurocodes, 2022.

CGNG: Règles NV 65, modifiées en décembre 1999, avril 2000 et février 2009 et annexes. DTU P 06-002 : Règles définissant les effets de la neige et du vent sur les constructions., Commission Générale de Normalisation du Bâtiment, 2000.

Dassault Systèmes: Abaqus/Standard. Version 11.2., Tech. rep., Providence, RI: Dassault Systèmes Simulia Corp., 2017.